# Hyperactive CREB subpopulations increase during therapy in pediatric B-lineage acute lymphoblastic leukemia

Dino Masic,[1] Kayleigh Fee,[2] Hayden L. Bell,[1] Marian Case,[1] Gabby Witherington,[1] Sophie Lansbury,[1] Juan Ojeda-Garcia,[3,4] David McDonald,[3,4] Claire Schwab,[1] Frederik W. van Delft,[1] Andrew Filby[3,4] and Julie Anne Elizabeth Irving[1]

[1]Wolfson Childhood Cancer Research Centre, Newcastle University Centre for Cancer, [2]Haematology Department, Flow Cytometry Laboratory, Royal Victoria Infirmary, [3]Newcastle University Flow Cytometry Core Facility, Newcastle University and [4]Innovation, Methodology and Application Research Theme, Newcastle University, Newcastle upon Tyne, UK

**Correspondence:** J. Irving
julie.irving@newcastle.ac.uk

**Received:** June 21, 2022.
**Accepted:** November 10, 2022.
**Early view:** November 24, 2022.

**https://doi.org/10.3324/haematol.2022.281177**

Supplementary Material for

# Hyperactive CREB subpopulations increase during therapy in paediatric B lineage acute lymphoblastic leukaemia

Dino Masic[1], Kayleigh Fee[2], Hayden Bell[1], Marian Case[1], Gabby Witherington[1], Sophie Lansbury[1], Juan Ojeda-Garcia[3,4] David McDonald[3,4], Claire Schwab[1], Frederik W van Delft[1], Andrew Filby[3,4] and Julie Anne Elizabeth Irving[1].

1. Wolfson Childhood Cancer Research Centre, Newcastle University Centre for Cancer, Newcastle upon Tyne, UK.
2. Haematology Department, Flow Cytometry Laboratory, Royal Victoria Infirmary, Newcastle upon Tyne, UK.
3. Newcastle University Flow Cytometry Core Facility, Newcastle University, Newcastle upon Tyne, UK.
4. Innovation, Methodology and Application Research Theme, Newcastle University, Newcastle upon Tyne, UK.

## Supplementary Methods

### Cell Staining

Antibodies were selected based on their ability to identify a leukaemia-associated immunophenotype to allow detection of MRD and normal B cells in all patients, enable exclusion of apoptotic cells, monitor cell proliferation and finally, identify phospho-signals of pathways that are recurrently activated in B lineage ALL. The Maxpar panel designer was used to designate metal tags (Fluidigm, San Francisco, USA). The full antibody panel is shown in Supplementary Table 4. Samples were stained for CyTOF analysis using a modified protocol acquired from Fluidigm. Briefly, $3x10^6$ cells were labelled with all antibodies, fixed in Maxpar Fix and Perm buffer (Fluidigm), stored overnight at 4ºC and acquired by mass cytometry the next day.
All antibodies were validated using appropriate positive and negative control cell lines with known CD antigen expression or by specific stimulation and/or inhibition of signalling pathways using specific small molecule inhibitors (Supplementary Table 5). Single antibody experiments also confirmed negligible signal spill over into other detectors.

### Mass Cytometry (CyTOF)

Sample counts and quality were checked on a BD Accuri flow cytometer and then, based on absolute cell count, adjusted to no more than $5 \times 10^5$/ml per sample in ultra-pure de-ionised water with the addition of 10% (v/v) EQ, four element calibration beads (Fluidigm, San Francisco, USA). Samples were then acquired on a fully calibrated/tuned Helios CyTOF machine (Fluidigm, San Francisco, USA) after filtration at 30µm to minimise blockages in the machine. The target number of cells was 50,000 for diagnostic samples and $1x10^6$ for follow-up samples. Down sampling of mass cytometry data showed that MMIs were similar from 10,000 to 100 and even 40 cells (data not shown), although only 2 samples had less than 50 ALL cells. Aliquots of normal peripheral blood processed and stained in an analogous fashion to the experimental samples were run at the start and end of each acquisition block to track signal variation over the duration of the run. Signals were normalised using the EQ beads as per the Fluidigm method [1] and transformed using the inverse hyperbolic sine (arsinh) function, with a cofactor of 5.

### Manual Gating

CyTOF data was analysed using both Cytobank (Santa Clara, USA) and FlowJo (Ashland, USA). Sequential gating was performed to identify live, single, ALL and mature B-cells. Firstly, control beads were gated out, singlets were identified using the 191Ir DNA marker and then apoptotic cells gated out if positive for 195Pt cisplatin [1], cleaved Caspase-3 or cleaved PARP (Supplementary figure 2). ALL cells and mature B-cells were then identified based on CD antigen expression; mature B-cells, by the immunophenotype, CD34- CD10-

CD22+ CD45+ and ALL cells by their LAIP, i.e. CD19+ CD10+/- CD34+/- and underexpression of CD45 and/or CD38 and/or overexpression of CD123 and/or CD58 [2]. MMI signals from ALL cells were normalised against internal mature B-cell populations by subtraction. Samples with less than 50 mature B-cells were normalised using the median values of mature B-cells from all samples. This was only necessary in 12 of 61 samples (8 presentation and 4 MRD samples).

**CyTOF Workflow**

The R pipeline CyTOF workflow (version 4) was used to computationally define cell populations using FlowSOM and ConsensusClusterPlus clustering, with data visualised using dimensional reduction technique, UMAP, among other graphical representations. Detailed methodology from [3] was followed. Matched presentation and MRD samples were pre-gated removing EQ beads, cells positive for cisplatin (dead), cCASPASE3 and / or cPARP (apoptotic). Samples were sequentially gated using LAIPs to select blast populations which were analysed using phospho-markers pCREB, pHH3, pp38, pAKT, pERK, pPLCg2, pS6, pSHP2, pSTAT4, pSTAT5, pZAP70, and pH2AX. CyTOF workflow was also used to graphically represent the differential cell population abundance between these matched populations. UMAP plots were generated using standard settings in the CyTOF workflow pipeline, with all gated cells used in the analysis. UMAPs were displayed by scaled expression of specific markers (scaling between 0 and 1 using percentile expression as the boundary), time point (Presentation or MRD), or designated cluster. Data was investigated for batch effect but no bias was identified (Supplementary Figure 5).

**Viability assays using Alamar Blue**

Cells were plated out in triplicate into flat bottomed 96-well plates and treated with the small molecule CREB inhibitor 666-15 (R and D systems, Abingdon, UK) diluted in DMSO, at a range of concentrations in standard media. PDX cells were maintained in RPMI-1640 supplemented with 20% FBS. After 96 hours, cytotoxicity was assessed using AlamarBlue Cell Viability Reagent (Thermofisher, Cramlington, UK) and fluorescence output measured at 560nM using a BMG Omega microplate reader. The replicate results were averaged and expressed as a percentage of the control vehicle (DMSO). Normalised results were plotted in GraphPad Prism software (GraphPad software Inc, San Diego, CA, USA) and fitted to a non-linear regression curve to estimate drug absolutes half-maximal inhibitory concentration ($IC_{50}$).

***Ex vivo* image-based drug response analysis**

Drug responses were assessed in primary and primary-derived ALL cell co-cultures with hTERT-immortalised bone marrow mesenchymal stromal cells (MSCs) in black-walled, 384-well plates (Greiner Bio-One, Stonehouse, UK; #781186). MSCs were seeded at 2.5 x $10^3$ per well in 50 μL RPMI-1640 supplemented with 10% FBS, left for 30 minutes at room temperature, then incubated at 37°C. Media was aspirated 24 hours later and approximately 3

x $10^4$ viable ALL cells from cryopreserved samples were added to each well in 25 μL serum-free AIM-V medium (ThermoFisher Scientific, UK). Following 24 hours co-culture, ALL cells were treated in technical triplicate with the small-molecule CREB inhibitor 666-15 (R&D Systems, Abingdon, UK) at indicated concentrations constituted in AIM-V medium (final DMSO concentration 0.1%). After 96 hours, co-cultured ALL cells and MSCs were stained with CyQUANT® Direct Cell Proliferation Assay (ThermoFisher Scientific, UK) nuclear stain, as per manufacturer's instructions.

Whole wells were imaged using an automated ZEISS CellDiscoverer 7 (Carl Zeiss AG, Oberkochen, Germany) equipped with an ORCA-Fusion camera (Hamamatsu Photonics K.K., Shizuoka, Japan) using a 5X Plan Apochromat objective and a 2X optovar, set to 37°C and 5% $CO_2$. A combined software autofocus and definite focusing strategy was used with a 20 ms exposure time in the 488/509 nm (ex/em) channel. Image acquisition was set to cover the entirety of each well with margins in a total of nine images saved in 16-bit TIF file format. For analysis, images were segmented using a supervised machine learning pipeline to enumerate and discriminate ALL cells and MSCs, developed with the Python programming language and two open-source applications [4,5]. For pixel-based classification, the random forest classifier was implemented from the sklearn.ensemble.RandomForestClassifier module of Scikit-learn [6]. Mean absolute live ALL and MSC replicate cell counts were expressed as a percentage of vehicle-treated cells (DMSO). Normalised results were again plotted and $IC_{50}$ values calculated.

## Supplementary Tables

## Table S1. Clinical details of patients and PDX in the study

| ID | Subgroup | Gender | Age at Pres (years) | Presentation WBC (x $10^9$/L) | MRD Level Day 28 (%) | EFS Status | Survival Status | Karyotype |
|---|---|---|---|---|---|---|---|---|
| L736 | dic(9;20) | F | 2 | 71.9 | UN | Continous CR | Alive | 48,XX,+X,dic(9;20)(p11~13;q11.21),+10,del(15)(q22),+21[7] |
| L784 | dic(9;20) | M | 8 | 55.8 | 0.00% | Continous CR | Alive | 45,XY,dic(9;20)(p11~13;q11) |
| LK131 | dic(9;20) | F | 3 | 36 | 0.00% | Continous CR | Alive | 47,XX,dic(9;20)(p13;q11.2),+21,inc[cp4] |
| LK169 | dic(9;20) | M | 3 | 15 | 0.00% | Continous CR | Alive | 47,XX,dic(9;20)(p13;q11.2),+21,+mar,inc[4] |
| LK286 | dic(9;20) | M | 2 | UN | 0.00% | Continous CR | Alive | 46,XY,dic(9;20)(p13;q11.2),add(7)(p11),+mar,inc[2] |
| LK85 | dic(9;20) | F | 11 | 20.1 | UN | UN | UN | 47,XX,+8,dic(9;20)(p13;q11.2),-13,+21c,+21[8] |
| L837 | ETV6-RUNX1 | F | 6 | 125 | 0.01% | Relapse | Alive | 48,XX,del(5)(q22q35),+10,+21[10] |
| L847 | ETV6-RUNX1 | F | 2 | 16.5 | 0.00% | Continous CR | Alive | 46,XX[10] |
| L997 | ETV6-RUNX1 | F | 2 | 62.4 | 0.00% | Continous CR | Alive | 46,XX[14] |
| LK160 | ETV6-RUNX1 | F | 2 | 109.1 | 0.00% | Continous CR | Alive | Fail |
| LK207 | ETV6-RUNX1 | F | 9 | 52 | 0.03% | Continous CR | Alive | 48,XX,add(9)(p2),add(12)(p12),+21,+mar,inc[cp3] |
| LK272 | ETV6-RUNX1 | M | 7 Months | UN | 0.47% | Continous CR | Alive | 46,XY,del(12)(p11.2p13)[8] |
| L835 | HeH | M | 4 | 7.8 | 0.36% | Continous CR | Alive | 53,XY,+X,+4,+10,+14,+17,+18,+21[6] |
| LK150 | HeH | M | 2 | UN | 0.04% | Continous CR | Alive | .nuc ish(DXZ1x3,ABL1x3,IGHx4,RUNX1x4)[~80%] |
| LK171 | HeH | M | 16 | 0.6 | 0.01% | Continous CR | Alive | 54~56,XY,+X,+4,+6,+9,+10,+14,+17,+18,+21,+21[cp3] |
| LK198 | HeH | M | 6 | 30.5 | 0.05% | Continous CR | Alive | .arr[hg19](4,6,14,17,21,X,Y)x3,(10p15.3q23.31)x3,(10q25.2q26.3)x3 |
| LK20 | HeH | M | 4 | 1.6 | 0.01% | Continous CR | Alive | 51~54,XY,+X,+4,+6,+14,+18,+21,+21[cp3] |
| LK231 | HeH | M | 3 | 9.6 | 0.24% | Continous CR | Alive | 62,inc[1]/46,XY[2] |
| L904 | iAMP21 | F | 14 | 5 | 3.39% | Relapse | Alive | 46,XX,t(2;16)(p12;q23),-21,+mar[5] |
| LK248 | iAMP21 | F | 8 | UN | 0.05% | Relapse | Dead | 46,XY,+X,del(4)(q25),del(9)(p21),del(11)(q13),add(14)(q32),-20,add(21)(q22)[8] |
| LK219 | IGH-CRLF2 | M | 1 | UN | UN | Continous CR | Alive | .nuc ish(IGHx2)(5'IGH sep 3'IGHx1)[88%]/(CRLF2x2)(5'CRLF2sep 3'CRLF2x1)[96%] |
| L727 | MLL Translocation | F | 1 | 94 | UN | Continous CR | Alive | 46,XX,t(11;12)(q23;q13)[7] |
| LK176 | MLL Translocation | M | 1 | 109.6 | 0.00% | Continous CR | Alive | 46,XY,t(11;17)(q23;p13)[7]/46,idem,del(9)(q13q22)[3] |
| L787 | Other | M | 19 | 7.7 | 26.70% | Relapse | Alive | 46,XY[20] |
| L792 | Other | M | 5 | 10.9 | UN | Continous CR | Alive | 46,XY,i(21)(q10)[2] |
| L839 | Other | M | 3 | 30 | 0.00% | Continous CR | Alive | 46,XY,-2,der(10)t(2;10)(q21;q22),+der(14)[3] |
| L844 | Other | M | 11 | 49 | 0.00% | Continous CR | Alive | 46,XY,add(9)(q34),i(9)(q10)[9] |
| L858 | Other | F | 14 | 33.9 | 0.03% | Continous CR | Alive | 46,XX[20] |
| L936 | Other | F | 2 | UN | 0.00% | Continous CR | Alive | UN |
| L955 | Other | F | 5 | UN | 0.01% | Continous CR | Alive | UN |
| L958 | Other | F | 9 | UN | UN | Continous CR | Alive | 47,XX,+21c[20] |
| LK82 | Other | M | 7 | 11.4 | 0.04% | Relapse | Alive | 46,XY,del(6)(q1q2),add(9)(p1),inc[4] |
| LK114 | Other | M | 9 | UN | 0.28% | UN | UN | UN |
| LK157 | Other | M | 3 | 121 | 0.00% | Continous CR | Alive | 53~55,XY,+X,+3,+6,+9,+14,+17,+18,+18,+21[cp8] |
| LK172 | Other | F | 4 | UN | 0.03% | Continous CR | Alive | 47,XX,t(6;20)(p25;q11.2),+22[9] |
| LK182 | Other | F | 5 | 13.4 | 0.00% | Continous CR | Alive | 46,XX[15] |
| LK196 | Other | M | 16 | 315.5 | 0.00% | Relapse | Dead | 46,XY[20].arr[hg19](9p21.3)x0,(14q32.33)x1 |
| LK221 | Other | F | 1 | 77.8 | UN | Continous CR | Alive | 46,XX[20] |
| LK275* | Other | F | 15 | UN | 51.50% | Continous CR | Alive | .nuc ish(PAX5x2)(5'PAX5 sep 3'PAX5x1)[66%]/(JAK2x2)(5'JAK2 sep3'JAK2x1)[58%] |
| L730 | t(1;19) | F | 11 | 86 | UN | Continous CR | Alive | 46,XX,der(19)t(1;19)(q23;p13)[4] |
| LK263 | t(1;19) | F | 7 | UN | 0.00% | Continous CR | Alive | 46,XX,der(19)t(1;19)(q23;p13.3)[7] |
| LK38 | t(1;19) | M | 4 | 28 | 0.00% | | | Fail |
| L707 PDX | TCF3/HLF | F | 16 | 39.1 | UN | UN | UN | 46,XX,der(19)t(17;19)(q22;p13)[12]/ 46,idem,fra(10)(q25)[17] |
| L829 (rel) PDX | HeH | F | 3 | 11.7 | UN | UN | UN | 51,XX,+X,+6,+14,+21,+21[2] |
| L920 PDX | Failed | F | 4 | 22.2 | UN | UN | UN | UN |

Patient cohort used throughout this study including group-based qualifier (L or LK number), confirmed cytogenetic subgroup, age at presentation, white blood cell count (WBC) at presentation, MRD percentage at end of induction (day 28), trial assigned to each patient (if known), and karyotype at diagnosis. UN= Unknown. PDX = Patient derived xenograft. * denotes identified PAX5-JAK2 translocation confirmed by fluorescent in situ hybridisation.

**Table S2. Clinical details of patients used in the paired presentation and MRD analyses.**

| ID | Subgroup | Gender | Age at Pres (years) | Presentation WBC (x $10^9$/L) | Karyotype | Time Point | MRD % by Flow Cytometry |
|---|---|---|---|---|---|---|---|
| L835 | HeH | M | 4 | UN | 53,XY,+X,+4,+10,+14,+17,+18,+21[6] | Presentation<br>Day 28 | 86.20%<br>0.36% |
| L936 | Other | F | 2 | UN | UN | Presentation<br>Day 28 | 76.00%<br>0.09% |
| LK20 | HeH | M | 4 | 1.6 | 51~54,XY,+X,+4,+6,+14,+18,+21,+21[cp3] | Presentation<br>Day 8 | 54.76%<br>17.50% |
| LK172 | Other | F | 4 | UN | 47,XX,t(6;20)(p25;q11.2),+22[9] | Presentation<br>Day 8 | 63.25%<br>17.55% |
| LK198 | HeH | M | 6 | 30.5 | .arr[hg19](4,6,14,17,21,X,Y)x3,(10p15.3q23.31)x3,(10q25.2q26.3)x3 | Presentation<br>Day 28 | 73.44%<br>0.05% |
| LK219 | IGH Translocation | M | 1 | UN | .nuc ish(IGHx2)(5'IGH sep 3'IGHx1)[88%]/(CRLF2x2)(5'CRLF2 sep 3'CRLF2x1)[96%] | Presentation<br>Day 8 | 50.50%<br>82.82% |
| LK231 | HeH | M | 3 | 9.6 | 62,inc[1]/46,XY[2] | Presentation<br>Day 28 | 7.55%<br>0.24% |
| LK248 | iAMP21 | F | 8 | UN | 46,XY,+X,del(4)(q25),del(9)(p21),del(11)(q13),add(14)(q32),-20,add(21)(q22)[8] | Presentation<br>Day 8<br>Day 28 | 66.33%<br>32.81%<br>0.05% |
| LK272 | ETV6-RUNX1 | M | 7 Months | UN | 46,XY,del(12)(p11.2p13)[8] | Presentation<br>Day 28 | 80.41%<br>0.47% |
| LK275 | Other | F | 15 | UN | .nuc ish(PAX5x2)(5'PAX5 sep 3'PAX5x1)[66%]/(JAK2x2)(5'JAK2 sep3'JAK2x1)[58%] | Presentation<br>Day 8<br>Day 28<br>Week 10<br>Week 16 | 78.14%<br>93.39%<br>51.50%<br>2.06%<br>0.06% |
| LK286 | dic(9;20) | M | 2 | UN | 46,XY,dic(9;20)(p13;q11.2),add(7)(p11),+mar,inc[2] | Presentation<br>Day 28 | 88.89%<br>1.02% |

UN - data are unknown.

**Table S3. MMI of mature B-cells presentation and 'on-treatment' bone marrow samples.**

| Antigen | MMI Pres | Range | MMI MRD | Range | p value |
|---|---|---|---|---|---|
| pp38 | 0.92 | 2.73 | 1.54 | 10.96 | 0.20 |
| pAKT | 4.12 | 98.45 | 0.93 | 3.21 | 0.45 |
| pCREB | 48.62 | 126.89 | 42.59 | 132.03 | 0.54 |
| pERK | 0.91 | 6.21 | 0.83 | 3.41 | 0.85 |
| pHH3 | 28.33 | 160.24 | 23.92 | 61.05 | 0.64 |
| pPLCg2 | 0.12 | 190.3 | 0.1 | 0.32 | 0.48 |
| pS6 | 5.76 | 43.59 | 3.17 | 10.67 | 0.26 |
| pSHP2 | 5.68 | 34.52 | 4.67 | 32.78 | 0.70 |
| pSTAT4 | 0.6 | 3.98 | 0.69 | 4.35 | 0.77 |
| pSTAT5 | 1.72 | 16.48 | 1.66 | 7.92 | 0.95 |
| pZAP70 | 0.18 | 0.54 | 0.26 | 1.72 | 0.28 |
| pH2AX | 3.64 | 13.05 | 5.67 | 20.01 | 0.12 |

MMI of mature B-cells in presentation and MRD samples. A paired, two tailed, t test was performed to assess differences in the MMI of antigens analysed.

**Table S4. Antibody panel for mass cytometry of B lineage ALL.**

| Label | Target | Antibody Clone |
|---|---|---|
| 89Y | CD45 | HI30 |
| 141Pr | pSHP2 [Y580] | D66F10 |
| 142Nd | Caspase 3 (Cleaved) | D3E9 |
| 143Nd | PARP (Cleaved) | F21-852 |
| 144Nd | CD38 | HIT2 |
| 147Sm | pHistone H2A.X [Ser139] | JBW301 |
| 150Nd | pStat5 [Y694] | 47 |
| 151Eu | CD123 (IL-3R) | 6H6 |
| 152Sm | pAkt [S473] | D9E |
| 156Gd | p-p38 [T180/Y182] | D3F9 |
| 158Gd | CD10 | HI10a |
| 159Tb | CD22 | HIB22 |
| 162Dy | pPLCg2 [pY759] | K86689.37 |
| 163Dy | CD34 | 581 |
| 165Ho | pCREB/ATF1 [S133] | 87G3 |
| 167Er | pERK 1/2 [T202/Y204] | D13.14.4E |
| 169Tm | CD19 | HIB19 |
| 171Yb | pZAP70 [Y319]/Syk [Y352] | 17a |
| 172Yb | pS6 [S235/S236] | N7548 |
| 174Yb | pStat4 [Y693] | 38/p-Stat4 |
| 175Lu | pHistone H3 [S28] | HTA28 |
| 176Yb | CD58 (LFA-3) | TS2/9 |
| 191Ir | Iridium | NA |
| 195Pt | Cisplatin | NA |

The antibody panel used for mass cytometry detailing metal isotope labels and antibody clones.

**Table S5. Validation of Signalling Antibodies.**

| Target Protein | Label | Cells used in validation | Stimulation |
|---|---|---|---|
| pSHP2 | 141Pr | Jurkat | 1μM Wortmannin, 15 mins at 37°C |
| cCaspase3 | 142Nd | Pre-B 697 | 500nM Dexamethasone, 48 hours at 37°C |
| cPARP | 143Nd | Pre-B 697 | 500nM Dexamethasone, 48 hours at 37°C |
| pHistone H2AX | 147Sm | Jurkat | 50μM Etoposide, 2 hours at 37°C |
| pSTAT5 | 150Nd | Jurkat | Pervanadate, 15 mins at 37°C |
| pAkt | 152Sm | Jurkat | 1μM Wortmannin, 2 hours at 37°C |
| p-p38 | 156Gd | PBMC | 40nM PMA, 10 mins at 37°C |
| pPLCγ2 | 162Dy | Ramos | Pervanadate, 15 mins at 37°C |
| pCREB | 165Ho | PBMC | 50nM PMA, 1μg/ml Ionomycin, 15 mins at 37°C |
| pERK1/2 | 167Er | PBMC | 40nM PMA,10 mins at 37°C |
| pZAP70/Syk | 171Yb | Jurkat | Pervanadate, 15 mins at 37°C |
| pS6 | 172Yb | PBMC | 50nM PMA, 30 mins at 37°C |
| pSTAT4 | 174Yb | Jurkat | Pervanadate, 15 mins at 37°C |
| pHistone H3 | 175Lu | Jurkat | 100nM Nocodazole, 24 hours at room temperature |

Pervanadate working solution was comprised of sodium orthovanadate (125μM) and hydrogen peroxide (530μM). PBMC- peripheral blood mononuclear cells.

**Supplementary Figures**

Figure S1. CONSORT diagram for the study.

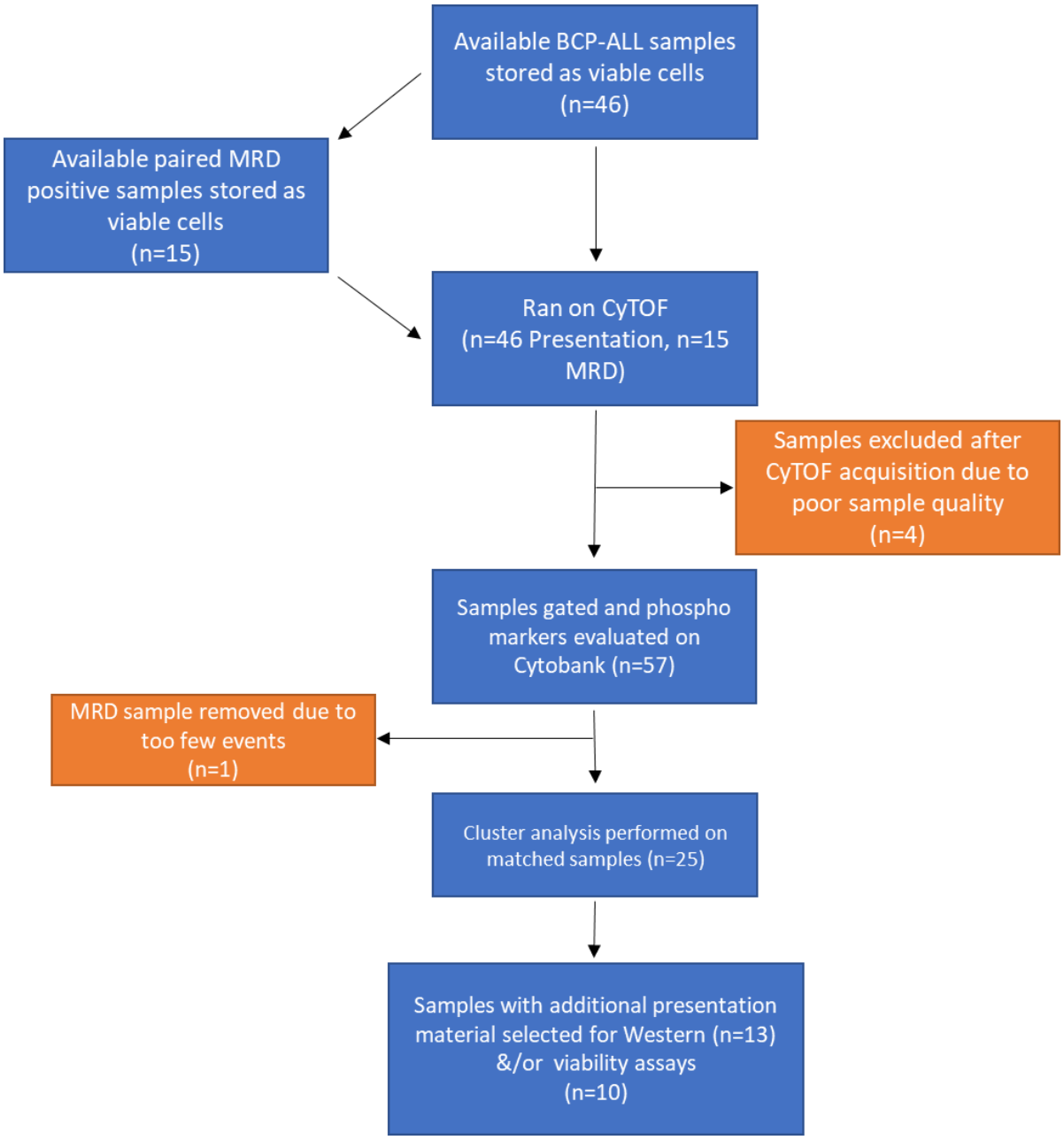

**Figure S2. Western analyses for pSTAT5 and pERK.**

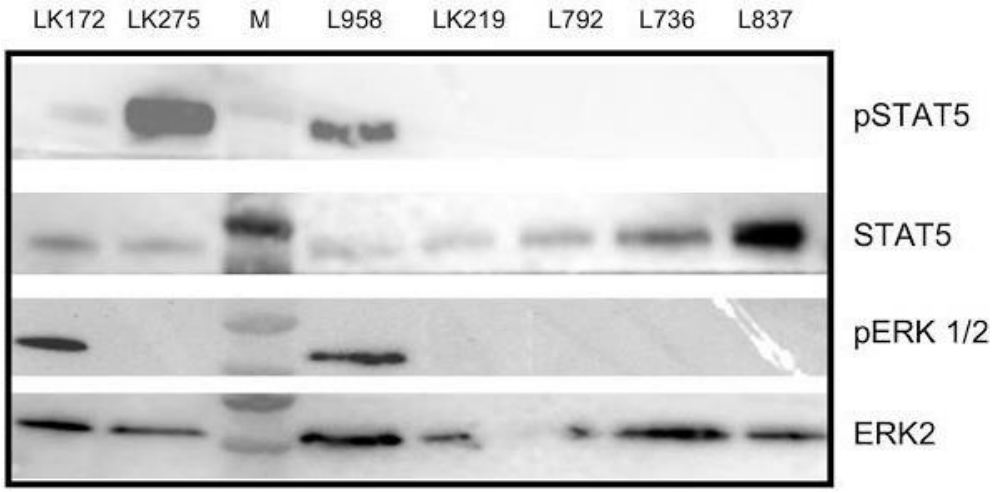


Western analysis of presentation ALL samples probed with antibodies to assess JAK-STAT and RAS pathway activation. M is the molecular weight marker lane. LK219 (pERK positive by CyTOF) had a low molecular weight band (not visible in figure) for pERK which may be due to sample degradation.

**Figure S3. Sequential gating protocol for BCP-ALL cells and mature B-cells**

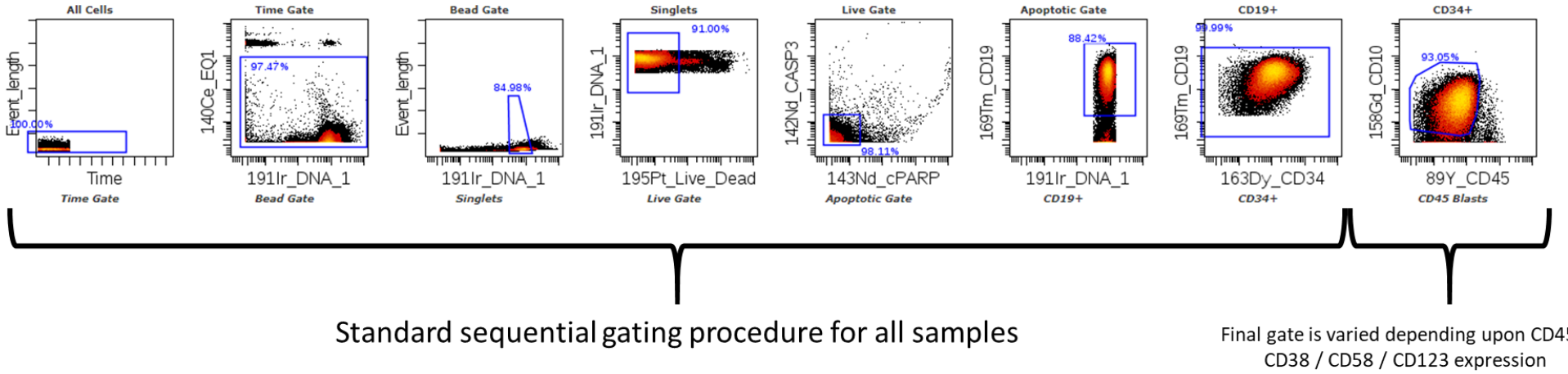


**B** Mature B-Cell Sequential Gating

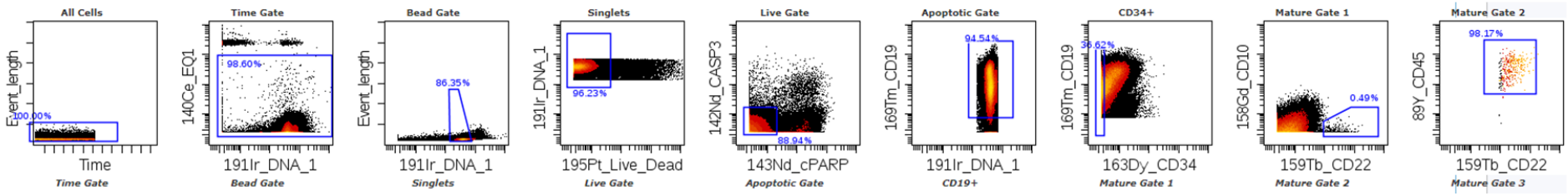


Sequential gating of cell populations. Gating first assesses acquisition of sample by analysing time against event length, allowing for the removal of aberrantly acquired cells that are a result of blockages. Next, EQ quality control beads are removed by gating out events positive for 140Ce. Singlets are then selected by assessing DNA against event length, removing debris and doublets. Next the viability marker cisplatin is used to separate dead cells from living. Dying cells are removed by selecting events negative for apoptotic markers cleaved CASPASE3 and cleaved PARP. At this stage only living healthy cells remain, from this population B lymphocytes are selected by gating for CD19+ events. CD34 heterogeneous cells are selected and a final marker, either CD45, CD38, CD58, or CD123 are used to identify leukaemic cells (A). Mature B-cells undergo identical initial gating, but CD34 negative cells are selected, followed by selection of CD10 negative/low and CD22 positive cells. A final gate is used, CD45 positive, CD22 positive cell population is selected to ensure only mature B-cells are selected (B).

**Figure S4. MRD levels by flow and mass cytometry are highly concordant**

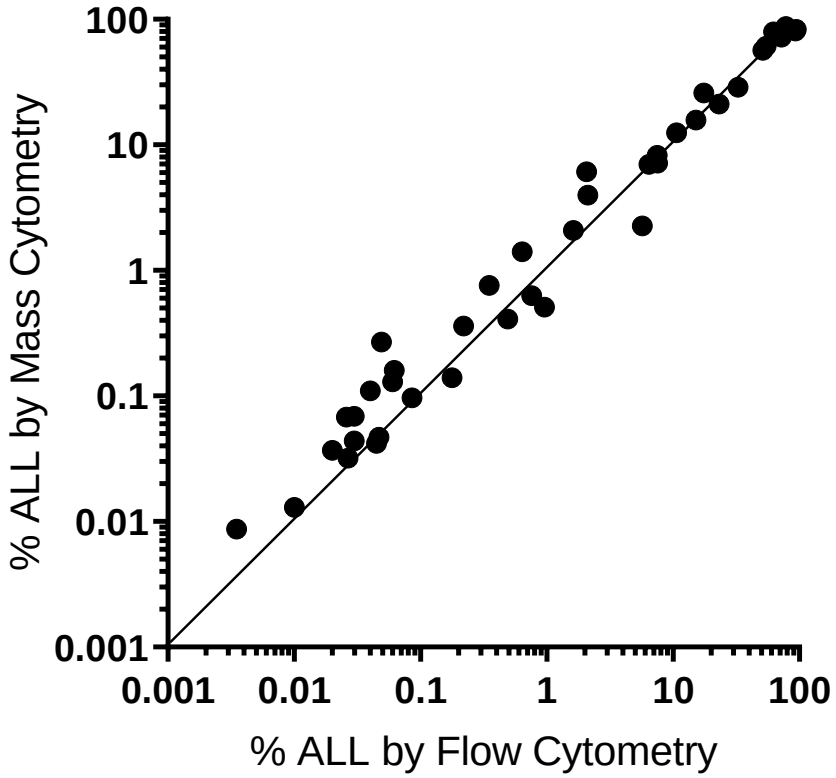


Bone marrow samples taken at disease presentation, or during induction therapy were processed and ALL cells quantified by both flow and mass cytometry using a standardised sequential gating strategy (n=45). Artificially created 'mock' MRD samples were also prepared (n=11) and included quality control MRD samples from an external quality assurance provider (n=9). The percentage of leukaemic cells ranged from 0.004% to 94.4%, with a mean of 17.71% and SD of +/-28%. Values were highly concordant between both technologies ($r^2$= 0.97).

**Figure S5. Modest induction of the CREB gene target, *CXCR4*, by dexamethasone.**

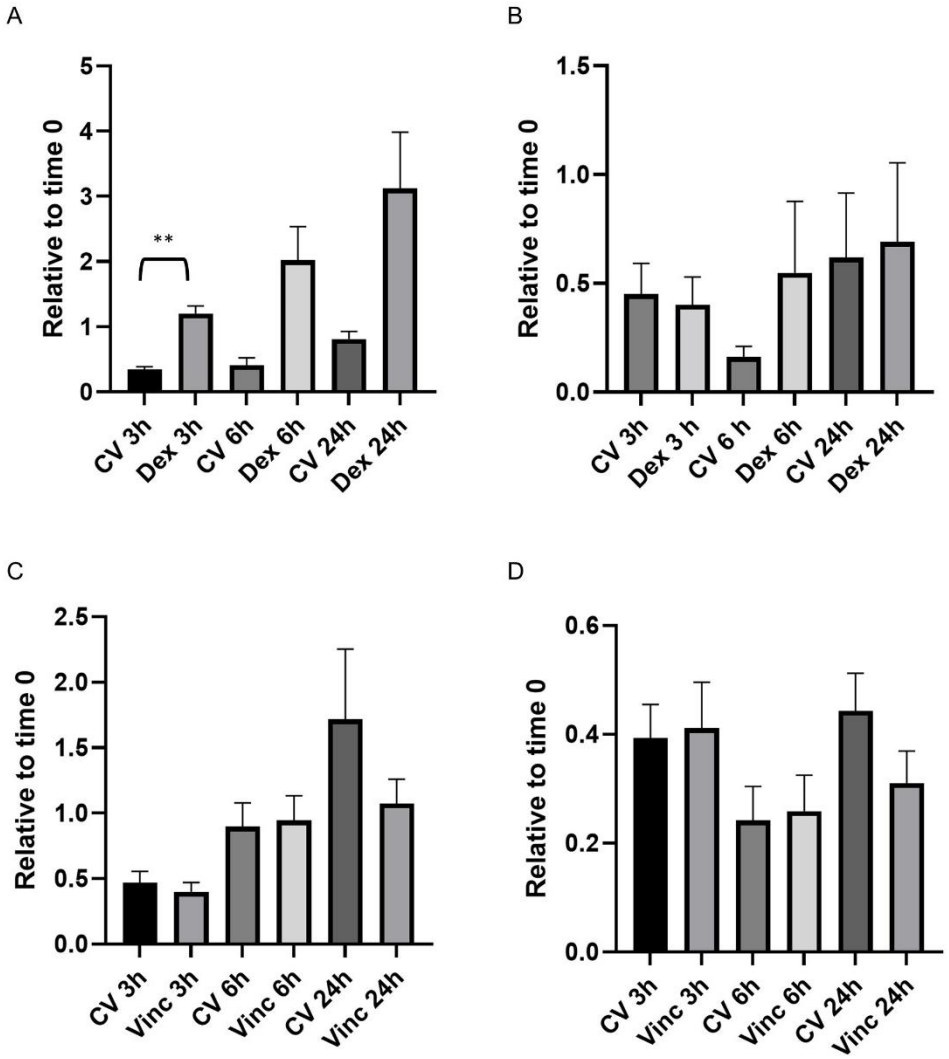


Histograms of *CXCR4* (A, C) and *MKNK2* (B and D) gene expression in PreB697 cells after dosing with $IC_{50}$ concentrations of dexamethasone, vincristine or CV for 3, 6 and 24 hours. Data are expressed relative to basal gene expression at time 0. Mean and SEM of 4 biological replicates are shown. ** denotes $p<0.01$.

**Figure S6. Batch effect analyses in gated leukemic cells and gated mature B-cells.**

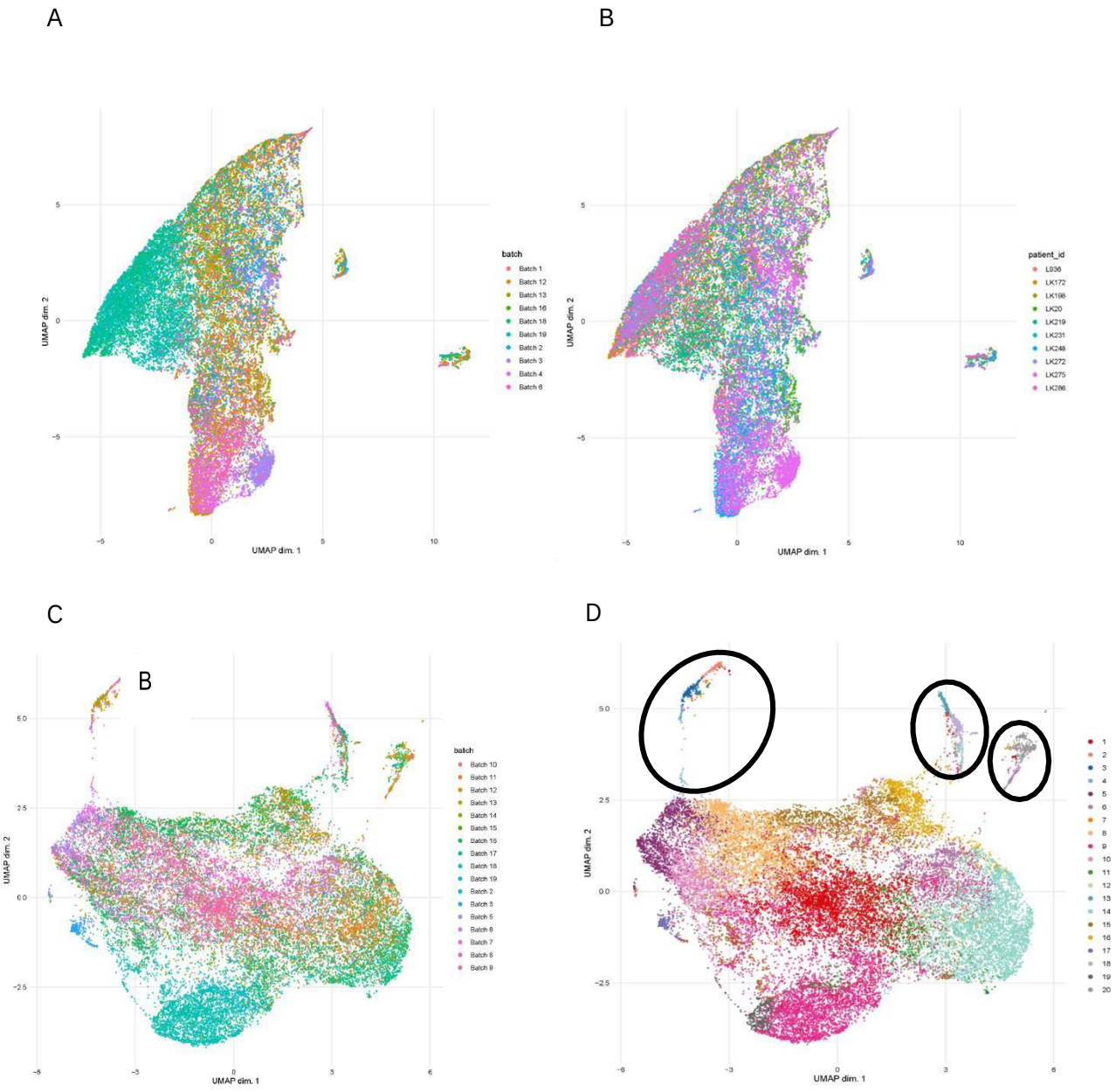

E

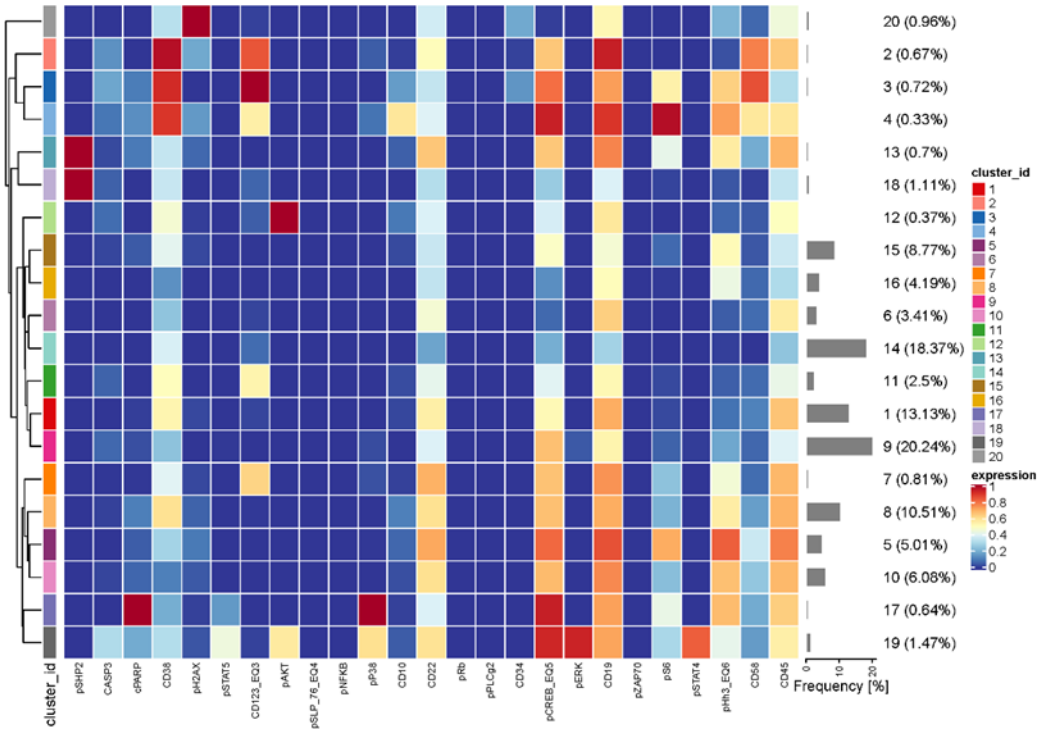


Batch effect testing on gated blast cells using UMAP. UMAP analysis of sample distribution showing a heterogeneous mix of batch (A) and patient samples (B). Investigation of gated mature B-cells shows negligible level of batching apart from batch 18 (C). The three islands separated from the main population of mature B-cells show biological rationale for separation. The top left island (1) is mainly populated from clusters 2, 3, and 4 which are characterised by high expression of CD123 and CD38. The top middle island (2) is predominantly populated by clusters 18 and 13 which are characterised by high pSHP2 expression. The right most island is predominantly populated by cluster 20 which is characterised by pH2AX indicating likely damaged cells (D). Heatmap showing signalling composition of each cluster (E).

## Supplementary References


1. Finck R, Simonds EF, Jager A, et al. Normalization of mass cytometry data with bead standards. *Cytometry A*. 2013;83(5):483-494.
2. Irving J, Jesson J, Virgo P, et al. Establishment and validation of a standard protocol for the detection of minimal residual disease in B lineage childhood acute lymphoblastic leukemia by flow cytometry in a multi-center setting. *Haematologica*. 2009;94(6):870-874.
3. Nowicka M, Krieg C, Crowell HL, et al. CyTOF workflow: differential discovery in high-throughput high-dimensional cytometry datasets. *F1000Res*. 2017;6:748.
4. Berg EL. Human Cell-Based in vitro Phenotypic Profiling for Drug Safety-Related Attrition. *Front Big Data*. 2019;2:47.
5. McQuin C, Goodman A, Chernyshev V, et al. CellProfiler 3.0: Next-generation image processing for biology. *PLoS Biol*. 2018;16(7):e2005970.
6. Pedregosa F, Varoquaux G, Gramfort A, et al. Scikit-learn: Machine Learning in Python. *Journal of Machine Learning Research*. 2011;12:2825-2830.